Novel ETV1 mutation in small cell lung cancer transformation resistant to EGFR tyrosine kinase inhibitors

Yan Zhou[1#], Hao Bai[1#], Jinjing Xia[1#], Wang-Yang Xu[2], Lei Cheng[1], Liwen Xiong[1]

[1]Pulmonary and Critical Care Medicine Department, Shanghai Chest Hospital, Shanghai Jiao Tong University, Shanghai, China; [2]Medical Department, Singlera Genomics (Shanghai) Ltd., Shanghai, China

Contributions: (I) Conception and design: L Xiong, Y Zhou; (II) Administrative support: L Xiong; (III) Provision of study materials or patients: H Bai, J Xia; (IV) Collection and assembly of data: WY Xu; (V) Data analysis and interpretation: L Cheng; (VI) Manuscript writing: All authors; (VII) Final approval of manuscript: All authors.

[#]These authors contributed equally to this work.

Correspondence to: Liwen Xiong. Shanghai Chest Hospital, Shanghai Jiao Tong University, 241 West Huaihai Road, Shanghai 200030, China. Email: Xiong_li_wen@126.com.

Background: Non-small cell lung cancer (NSCLC) patients harboring mutations in the epidermal growth factor receptor (*EGFR*) gene respond dramatically to *EGFR* tyrosine kinase inhibitors (TKIs). However, these patients inevitably develop acquired resistance to *EGFR*-TKIs. Among them, small cell lung cancer (SCLC) transformation is a relatively rare mechanism.

Methods: We used a 639 cancer-relevant gene panel to detect genetic differences in tissues before and after *EGFR*-TKIs resistance caused by SCLC transformation. *In vitro* experiments were conducted to study the role of ETS variant transcription factor 1 (*ETV1*) on SCLC transformation and *EGFR*-TKIs resistance.

Results: We present two *EGFR*-mutant lung adenocarcinoma (LUAD) patients. One patient, with *EGFR* exon 19 deletion (Ex19del), accepted first-line gefitinib treatment and then received osimertinib treatment due to acquisition of an *EGFR*-T790M mutation. A novel *ETV1* mutation (p.P159S) was detected in the SCLC tissue after osimertinib resistance when not coexisting with T790M. The other patient harbored an *EGFR* exon 21 mutation (p.L858R), and had a long-lasting response to first-line gefitinib, and then transformed to SCLC after TKI resistance. A previously unreported *ETV1* mutation (p.E462Q) was detected in the SCLC tissue. *In vitro*, *ETV1* p.E462Q and p.P159S mutations participated in neuroendocrine differentiation by inducing the expression of achaete-scute homolog 1 (ASCL1) and promoting the proliferation of H69 cells. *ETV1* p.E462Q and p.P159S mutations were also resistant to gefitinib and osimertinib after introduction into H358 cells.

Conclusions: Novel *ETV1* p.E462Q and p.P159S mutations were found in the SCLC tissues of TKIs-resistant LUAD patients, providing a new understanding of *ETV1* involvement in acquired resistance to *EGFR*-TKIs via SCLC transformation.

Keywords: *ETV1*; non-small cell lung cancer (NSCLC); small cell lung cancer transformation (SCLC transformation); *EGFR* tyrosine kinase inhibitor (*EGFR* TKI); drug resistance

Submitted Apr 27, 2021. Accepted for publication Jul 07, 2021.
doi: 10.21037/atm-21-2625
View this article at: https://dx.doi.org/10.21037/atm-21-2625

Introduction

Non-small cell lung cancer (NSCLC), which accounts for the majority of lung cancer cases, is one of the most common malignant tumors in the world (1,2). Most of the patients are in advanced stage at the time of diagnosis, and those that harbor sensitive mutations could receive targeted therapies as the standard treatment. The most common epidermal growth factor receptor (*EGFR*) mutations are

© Annals of Translational Medicine. All rights reserved.

exon 19 (Ex19del) or exon 21 (L858R) (3). The use of first-line *EGFR*-tyrosine kinase inhibitors (TKIs) such as gefitinib, erlotinib (first-generation), and afatinib (second-generation), which represent the standard treatment of advanced *EGFR*-mutated NSCLC, dramatically improves the prognosis of patients (4). However, after a median of 8–12 months of treatment, the disease will often progress, which indicates acquired resistance to *EGFR*-TKIs (5). The mechanisms of acquired drug resistance comprise *EGFR* T790M mutation, *c-Met* and *HER2* amplification, and other driver gene mutations, as well as histological transformation to small cell lung cancer (SCLC) and an epithelial-mesenchymal (EMT) phenotype (6). Osimertinib (AZD9291) is the third generation of *EGFR*-TKIs, which has been shown to be effective in NSCLC patients with T790M mutation, however most patients will also inevitably develop drug resistance (7,8). Acquired *EGFR* C797S mutation is one of the most common osimertinib-resistant mechanisms, and SCLC transformation has also been reported (9-11).

Studies have shown that TKIs-resistant SCLC basically retains the original *EGFR* mutations, supporting the view that SCLC is not an independent second primary cancer, while *EGFR* mutations after SCLC transformation are not sensitive to *EGFR*-TKIs (12). Moreover, the majority of patients with histologically transformed SCLC were female non-smokers, which differed from the clinical manifestations of primary SCLC patients. These studies hypothesized that SCLC and NSCLC may have common origin cells despite their different biological and genomic characteristics (12-14). SCLC transformation is always associated with inactivating mutations in the *RB1* and *TP53* genes (15). Other alterations such as *PTEN*, *CREBBP*, *SLIT2*, *EP300*, and *MLL* mutations, as well as *FGFR1* amplification have also been found in SCLC transformation cases. Although these distinctive mechanisms are well-known, a heterogeneity of the resistance to TKIs in individual is still under study and requires more attention.

Herein, we investigated two patients with *EGFR*-mutant lung adenocarcinoma (LUAD) who had a long-lasting response to gefitinib or osimertinib treatment and developed resistance to *EGFR*-TKIs due to SCLC transformation. We used a customized 639 cancer-related genes panel to analyze the genetic background of the tumor samples before *EGFR*-TKI treatment and after SCLC transformation, and detected novel *ETV1* mutations in SCLC tissues. *In vitro* experiments showed that *ETV1* mutations regulated achaete-scute homolog 1 (ASCL1) levels and conferred resistance to gefitinib and osimertinib, providing new insights into the role of *ETV1* in lung tumorigenesis and histological transformation. This is the first report of a patient whose lung cancer transformed to SCLC after *EGFR*-TKI therapy with an acquired *ETV1* mutations, which provides new insight into the function of the *ETV1* gene and identifies a potential target that can be included in future treatment strategies for this type of cancer.

We present the following article in accordance with the MDAR reporting checklist (available at https://dx.doi.org/10.21037/atm-21-2625).

Methods

Patients and sample collection

Two NSCLC patients with *EGFR* sensitive mutations were recruited from the Shanghai Chest Hospital. A real-world study was conducted to detect genetic changes in the SCLC transformation after *EGFR*-TKI treatment. All procedures performed in this study involving human participants were in accordance with the Declaration of Helsinki (as revised in 2013). The study was approved by Research Ethics Committee of Shanghai Chest Hospital (IS2118) and informed consent was taken from all the patients. Clinical information including age at diagnosis, gender, tumor histology, clinical treatment approach, outcomes, and smoking status was collected. Formalin-fixed paraffin-embedded (FFPE) tumor tissues or fresh biopsy tissues were obtained. Histological types and tumor cell contents were confirmed by two pulmonary pathologists. The efficacy assessment which is divided into complete response (CR), partial response (PR), stable disease (SD) and progressive disease (PD) was evaluated using dedicated computed tomography imaging performed and evaluated by investigator according to the Response Evaluation Criteria in Solid Tumors (RECIST 1.1).

Targeted next-generation sequencing (NGS) and bioinformatics analysis

Germline DNA (gDNA) from fresh tissues or FFPE samples de-paraffinized with xylene were extracted by using the QIAamp DNA FFPE Tissue Kit (Qiagen, Hilden, Germany) according to the manufacturer's instructions. Sequencing libraries were prepared using the Illumina standard library (Illumina, Inc., California, USA) according to the

© Annals of Translational Medicine. All rights reserved.

manufacturer's protocols. Captured libraries were quantified by using the KAPA SYBR® FAST universal qPCR Kits (KAPA Biosystems, Boston, USA). The libraries were paired-end sequenced on an Illumina Miseq sequencer (Illumina, Hayward, CA, USA). A panel containing 639 cancer-related mutational hot genes (Singlera Genomics Inc., Shanghai, China) was used to detect multiple types of genomic variants, such as single-nucleotide variants, insertions, deletions, copy number variations, and rearrangements. The 639 involved genes are listed in Table S1.

Sequencing data were uploaded for filtering high quality reads, and clean data were aligned to The University of California at Santa Cruz (UCSC) human reference genome (GRCh37/hg19). Single-nucleotide variants, insertions or deletions, and amino acid changes were annotated by using the SnpEff (http://snpeff.sourceforge.net/). Variations detected in tumor tissues but not detected in matched blood were deemed as somatic alterations. Mutations with allele frequency >5% were defined as novel mutations. The I-TASSER server (http://zhanglab.ccmb.med.umich.edu/I-TASSER) was used to model the structure of *ETV1*.

Cells and reagents

The NCL-H358 cells (RRID: CVCL_1559) were maintained in RPMI1640 medium (Gibco BRL, Grand Island, NY, USA) supplemented with 10% fetal bovine serum (FBS, Gibco BRL, Grand Island, NY, USA) and 10 ng/mL of mouse IL3 (Cell Signaling Technology). NCL-H69 cells (RRID: CVCL_1579) were maintained in RPMI1640 medium (Gibco BRL, Grand Island, NY, USA) supplemented with 10% FBS (Gibco BRL). All cells were cultured at 37 ℃ in a 5% CO_2-humidified atmosphere. Gefitinib and Osimertinib were purchased from Selleck Chemicals (Houston, TX, USA).

Plasmid construction

A full-length cDNA fragment of human *EGFR* containing activating mutations (p.L858R and p.T790M) and a full-length cDNA fragment of human *ETV1* containing activating mutations (p.P159S and p.E462Q) were generated by Asia-Vector Biotechnology (Shanghai) Co. LTD. All mutated full-length *EGFR* or *ETV1* cDNAs were induced into the PCDNA3.1 vector (Asia-Vector Biotechnology, Shanghai, China) and confirmed by direct sequencing. The sequences for mutagenesis primers are listed in Table S2.

Cell growth inhibition assay

A total of 10^4 transfected H358 cells expressing different *EGFR*-mutant variants were plated in each well of a 96-well plate, which were grown in RPMI1640 medium. Next, dimethyl sulfoxide (DMSO) or *EGFR*-TKIs were added at the indicated drug doses, and the cells were cultured for 72 hours. The inhibitory effects of gefitinib and osimertinib on cell growth were detected using the Cell Counting Kit-8 reagent (BBI Life Sciences, Shanghai, China). Each experiment was performed in triplicate.

Proliferation assay

A total of 10^4 cells were plated in each well of a 96-well plate and grown in RPMI1640 medium with 10% FBS. At the indicated times points, the cell proliferation rate was detected using the Cell Counting Kit-8 reagent (BBI Life Sciences, Shanghai, China) according to the manufacturer's protocol. The number of viable cells was counted, and the proliferation plot was drawn using GraphPad Prism 8.0 software (GraphPad Software Inc. San Diego, CA, USA). Each experiment was performed in triplicate.

Quantitative reverse transcription PCR (qRT-PCR)

Total ribonucleic acid (RNA) was extracted using Trizol reagent (Invitrogen, CA, USA), and was then reverse transcribed into cDNA using the reverse transcriptase reagent kit (TaKaRa, Shiga, Japan). Quantitative PCR was performed using SYBR green PCR kit (TaKaRa, Shiga, Japan). Relative transcript quantities were analyzed using the ΔΔ cycle threshold (ΔΔCT) method and CT values were normalized to the CT value of the *GAPDH* gene. Data from each experiment was then normalized to the wild-type (WT) group to detect the relative expression changes in messenger RNA (mRNA). Each experiment was performed in triplicate. The sequences of primers are listed in Table S2.

Statistical analysis

For *in vitro* experiments, quantitative data were presented as mean ± standard errors of the mean. A two-tailed Student *t*-test was performed to calculate the statistically significant differences between two groups. A P value <0.05 was considered statistically significant. For all figures: asterisk (*)

© Annals of Translational Medicine. All rights reserved.

Table 1 Clinical characteristics of the two patients

Patient No.	Age	Gender	TNM stage	Primary tumor location	Smoking history	First biopsy: mutations (pathology)	TKI treatment	Second biopsy: mutations (pathology)	TKI treatment (second)	Third biopsy: mutations (pathology)
1	56	Male	T4N2M1	Right	No	EGFR exon19del (LUAD)	Gefitinib	EGFR exon19del/ T790M (LUAD)	Osimertinib	EGFR exon19del ETV1 E462Q (SCLC)
2	58	Male	T1aN2M1c	Left	No	EGFR L858R (LUAD)	Gefitinib	EGFR L858R ETV1 P159S (SCLC)	–	–

means P value <0.05, (**) means P value <0.01, (***) means P value <0.001.

Results

Patient's description

We report that two patients diagnosed with LUAD carrying *EGFR* activating mutations received *EGFR*-TKIs. Nonetheless, the patients progressed and tissue re-biopsies immediately following progression revealed a switch to SCLC histology. The clinical characteristics of the two individuals are shown in *Table 1*.

Case 1

A 56-year-old male, who never smoked, had intermittent hemoptysis for 5 months. Computed tomography (CT) showed an enlarged pleural mass in the inferior lobe of the right lung (4.3 cm × 2.9 cm) and multiple small nodules in bilateral lungs (*Figure 1A*). The pathological diagnosis was LUAD stage IV (T4N2M1), and immunohistochemical staining (IHC) confirmed the histology of pulmonary LUAD [pan cytokeratin positive (CK)+, thyroid transcription factor-1 positive (TTF1)+, cluster of differentiation 56 (CD56)–, and Ki-67 60%]. The molecular pathology results showed *EGFR* exon 19 deletion (2235_2249del/E746_A750del). This patient began first-line treatment with gefitinib 250 mg, once a day orally. CT scans showed a response after three months of treatment, and gefitinib was continued for a total of 12.5 months until the patient developed right pleural effusion (*Figure 1A*).

Subsequently, an *EGFR* T790M mutation was detected via the 639 DNA panel, and IHC showed CD56–, CK+, TTF1+, and NapsinA+ in the second biopsy specimen (Figure S1A). Osimertinib 80 mg, once daily orally, was then administered. After 4 months, osimertinib was permanently discontinued because of multiple localized pleural thickening on the right side of the lung (*Figure 1A*). A re-biopsy (third biopsy) was then performed, and this tumor was diagnosed as SCLC with a pathological stage of IV (T4N2M1) according to the World Health Organization (WHO) 2015 classification of lung tumors. IHC showed CD56+, CK+/–, TTF1+ (partial), NapsinA–, and synaptophysin+ (Figure S1B). Molecular analysis revealed novel genetic alterations different from those detected in previous biopsies, such as the *ETV1* p.E462Q mutation. The patient then received standard carboplatin (350 mg) and etoposide (100 mg/day ×5 days) therapy. After four cycles of this combined treatment, the patient exhibited disease progression and gradual increase of pleural effusion (*Figure 1A*).

Case 2

A 58-year-old man with no smoking history, complained of cough, sputum, and bone pain at his primary hospital. CT showed a 1.6 cm mass in the upper lobe of the left lung, bilateral pleural thickening, and uneven bone mineral density of the left scapula and part of the vertebral body (*Figure 1B*). Positron emission tomography-CT (PET-CT) revealed multiple lymph node metastases in the mediastinum, left hilum, and armpit, as well as bone metastasis. A CT-guided biopsy from the primary lesion was performed and diagnosed as LUAD with a pathological stage of IV (T1aN2M1c). IHC showed CD56–, CK+, and TTF1+ (Figure S1C). EGFR L858R was positively detected by NGS, and gefitinib 250 mg, once daily orally, was administered as the first-line therapy, resulting in a partial response (PR) (*Figure 1B*).

After 64 months, the left pleural dissemination began to grow (*Figure 1B*). After hospitalization, re-biopsy was performed from the pleural tumor near the left diaphragm, and transformation to SCLC with a pathological stage of IV (T2aN2M1c) was confirmed. IHC showed CD56+, CK+, TTF1+, and NapsinA+ (Figure S1D). T790M was not

© Annals of Translational Medicine. All rights reserved.

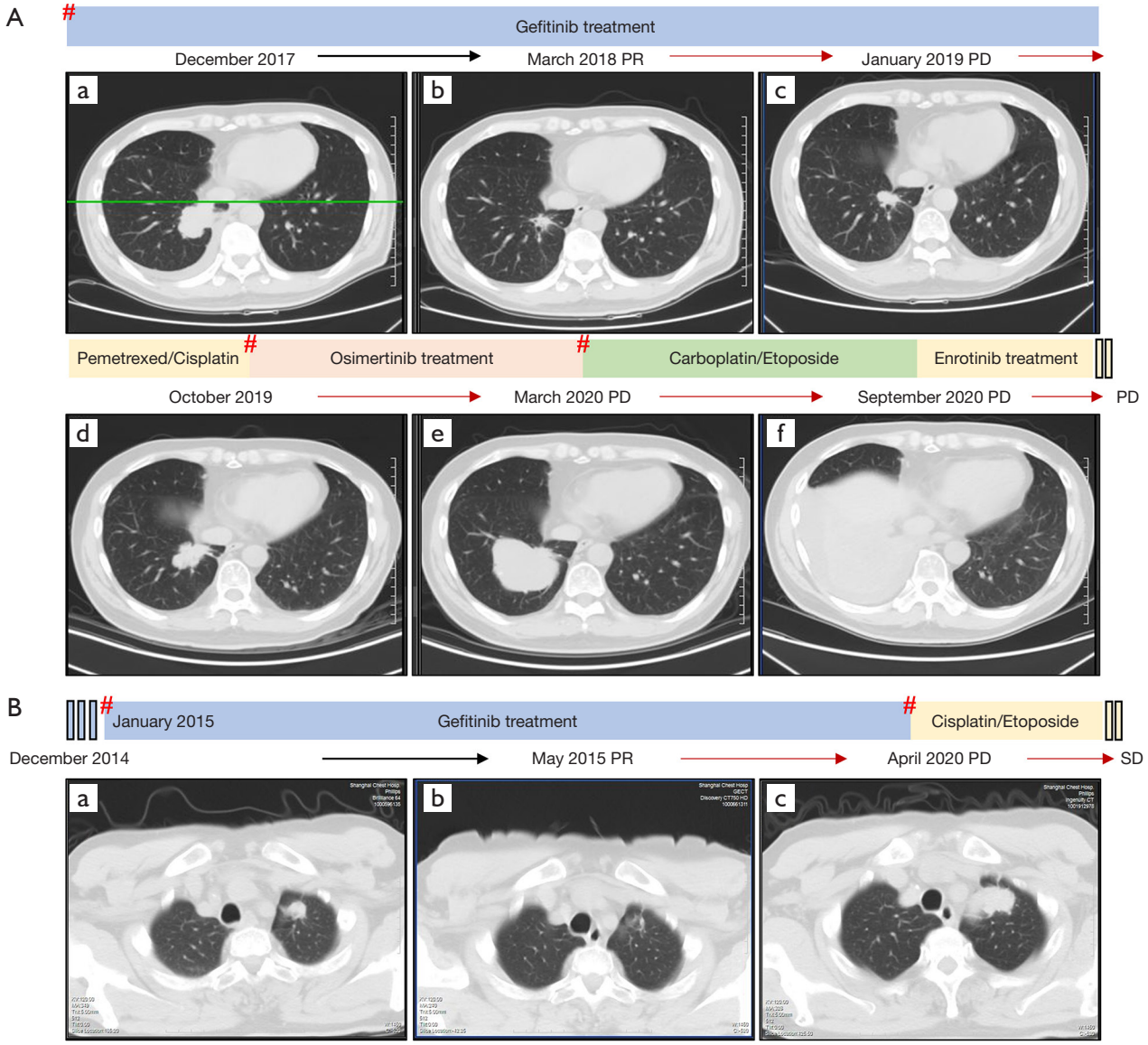

Figure 1 Tumor lesions detected by CT during the courses of the patients' diseases and treatment. (A) Case 1: (a) Before start of *EGFR*-TKI treatment. NGS showed *EGFR* exon 19 deletion. (b) PR after gefitinib treatment. (c) First progression after 12.5 months of gefitinib. (d) PD after 9 months of chemotherapy. *EGFR* T790M was detected. (e) Second progression after 4 months of osimertinib treatment. Appearance of the transformation to SCLC. *ETV1* p.E462Q was detected. (f) PD after 6 months of chemotherapy. (B) Case 2: (a) Before start of *EGFR*-TKI treatment. *EGFR* L858R was detected. (b) PR after 4 months of gefitinib treatment. (c) PD after 64 months of gefitinib treatment. *ETV1* p.P159S was detected. # represents the time point of NGS detection. NGS, next-generation sequencing; SCLC, small cell lung cancer; PR, partial response; PD, progressive disease.

detected in the tissue, however the novel *ETV1* mutation (ETV1 p.P159S) was, as in the SCLC tissue analysis of patient 1. Treatment was then changed to chemotherapy (cisplatin 100 mg + etoposide 100 mg/day ×5 days), which has been used until now.

Mutational analysis of ETV1

ETV1, which is located in 7p21.2, contains 21 exons and encodes a member of the ETS (E twenty-six) family of transcription factors. ETS transcription factors can directly bind to specific DNA sequences in the promoter/enhancer

© Annals of Translational Medicine. All rights reserved.

regions of genes to regulate various biological processes (16). The Cancer Genome Atlas (TCGA) database showed that *ETV1* mutations were most common in skin cancer, bladder urothelial cancer, nerve sheath tumor, prostate adenocarcinoma, melanoma, and endometrial carcinoma (*Figure 2A*). Point mutations reported in tumors were scattered in *ETV1* (*Figure 2B*). The mutation frequency of *ETV1* in LUAD and SCLC was 3.64% and 0.84%, respectively (*Figure 2C*,*D*). The mutation frequency of *ETV1* reported in the Asian population with LUAD was 1.37%, while that of European and Latin American populations was 2.73% and 1.71%, respectively. The point mutations of *ETV1* of LUAD were mainly concentrated in the EST-PEA3-N domain (*Figure 2E*).

In TCGA database, only three SCLC patients were reported to have *ETV1* mutation, and all of them were *ETV1* S100G (*Figure 2E*). The ethnic origin of samples with *ETV1* mutations in SCLC is unknown. Survival analysis showed that patients with *ETV1* mutations had a worse overall survival (OS) trend than those without *ETV1* mutations, although this was not statistically significant (Figure S2A). However, no differences were observed in progression-free survival (PFS) (Figure S2B). The worse OS trend of LUAD patients with *ETV1* mutations was obvious (Figure S2C), and the disease-free survival (DFS) of these patients was significantly shortened compared to LUAD patients without *ETV1* mutations (Figure S2D). SCLC patients had insufficient data to show the correlation between *ETV1* mutations and survival.

Clinical correlation analysis indicated that *ETV1* mutations were significantly associated with advanced Tumor Node Metastasis (TNM) stages of LUAD (P=0.038) (Figure S3A). *ETV1* mutations were more common in never-smoking LUAD patients (Figure S3B). In this study, the novel *ETV1* mutations identified in two cases were *ETV1* Pro159Ser (P159S), which was located in EST-PEA3-N domain, and Glu462Gln (E462Q), which was not located in a common functional domain (*Figure 3A*). Both of them changed the structures of the protein by computer simulation (*Figure 3B*,*C*), illustrating an important role of ETV1 in the development of lung cancer that has not been previously reported.

ETV1 mutations induced ASCL1 expression in SCLC

To ascertain whether ETV1 participated in neuroendocrine differentiation through regulating the expression of ASCL1, we transfected *ETV1* mutant plasmids into H69 cells. We found that there was no significant difference in the expression of ETV1 mRNA (*Figure 4A*), while *ETV1* p.E462Q and p.P159S mutant plasmids increased the ASCL1 mRNA levels after transfection (*Figure 4B*). We discovered that *ETV1* mutations indirectly inhibited *HES1* transcription (*Figure 4C*).

ETV1 mutations promoted SCLC proliferation in vitro

We infected H69 cells with mutant *ETV1* plasmids and found that *ETV1* p.E462Q and p.P159S mutations promoted SCLC proliferation *in vitro*. On the 2nd day after transfection, we observed that *ETV1* p.E462Q and p.P159S mutations markedly induced the proliferation of tumor cells (*Figure 4D*).

ETV1 p.E462Q and p.P159S mutations conferred resistance to gefitinib and osimertinib in vitro

We next determined whether *ETV1* p.E462Q and p.P159S mutations contributed to *EGFR*-TKI resistance. We transfected plasmids harboring *EGFR* L858R or T790M (in cis) with or without *ETV1* p.E462Q or p.P159S mutations into H358 cells, and exposed these cells to increased doses of osimertinib or gefitinib. As expected, cells expressing the *EGFR* L858R mutation were sensitive to gefitinib and osimertinib, with an IC50 of 241.8 and 160.3 nM, respectively (*Figure 5A*,*B*). Cells containing *EGFR* T790M were sensitive to osimertinib. *EGFR* mutant cells transfected with the *ETV1* p.P159S mutant variant exhibited a strong resistance to osimertinib. In cells exposed to increased doses of gefitinib, the *ETV1* p.E462Q and p.E462Q mutant variants exhibited a strong resistance to gefitinib when *EGFR* T790M was negative (*Figure 5C*).

Discussion

A large number of advanced NSCLC patients with *EGFR* mutations exhibit a good response to *EGFR*-TKIs. However, most patients develop resistance after an average of 8–14 months, caused by various alterations including *EGFR* T790M mutation, *EGFR* amplification, *MET* and *HER2* amplification, and *PIK3CA* mutations (13). Furthermore, 5–15% of NSCLC tumors will transform into SCLC histology (13,17). Acquired resistance is the main problem that limits the clinical effect of targeted treatment with *EGFR*-TKIs. Although the response of transformed SCLC to chemotherapy is good, the prognosis

© Annals of Translational Medicine. All rights reserved.

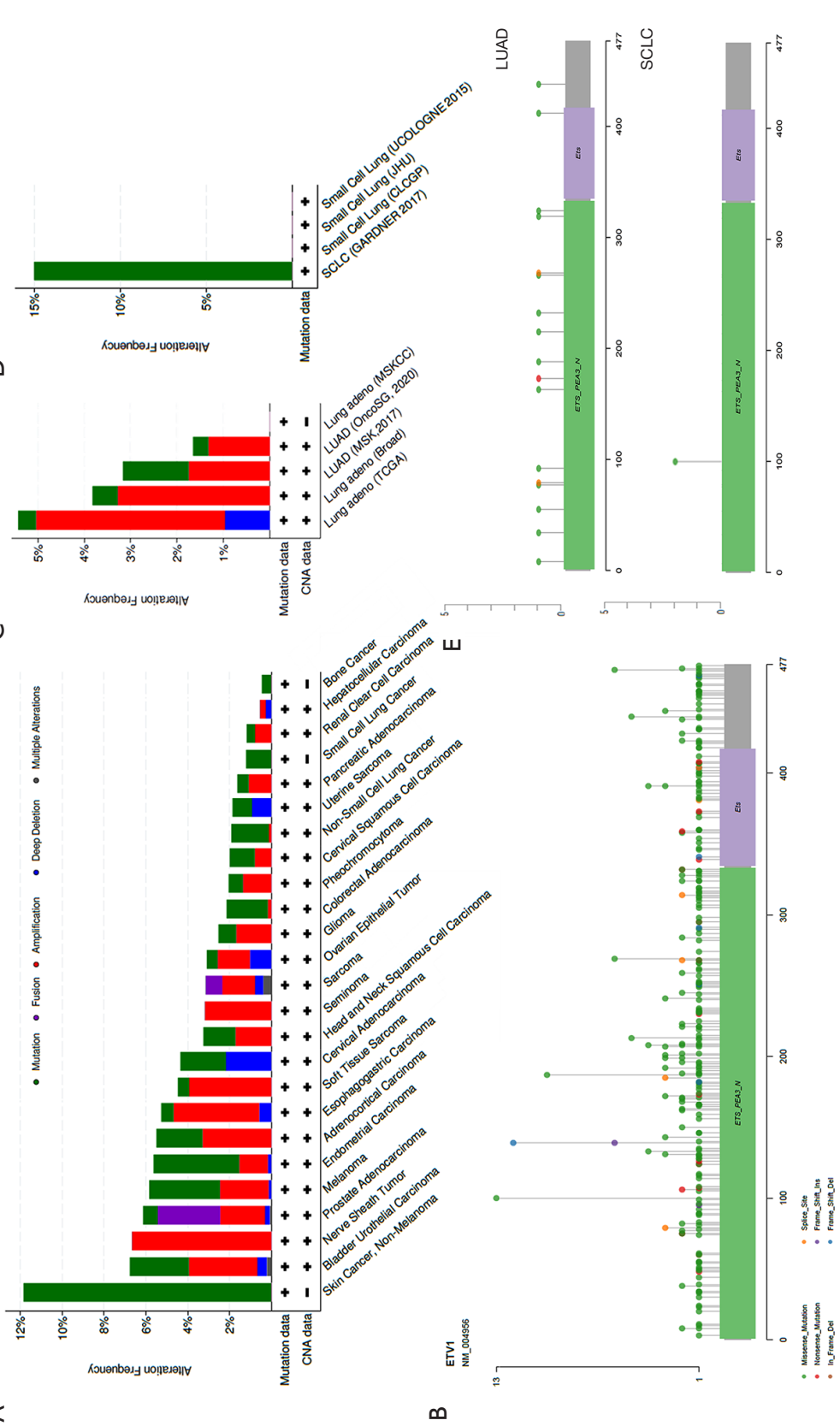

Figure 2 *ETV1* mutations in multiple tumors analyzed from TCGA database. (A) Thirty tumor types with the highest *ETV1* mutation frequency. (B) *ETV1* mutation sites and variation types. (C,D) Frequency and variation types of *ETV1* in LUAD and SCLC. (E) *ETV1* mutation sites in LUAD (upper) and SCLC (below). TCGA, The Cancer Genome Atlas; SCLC, small cell lung cancer; LUAD, lung adenocarcinoma.

© Annals of Translational Medicine. All rights reserved.

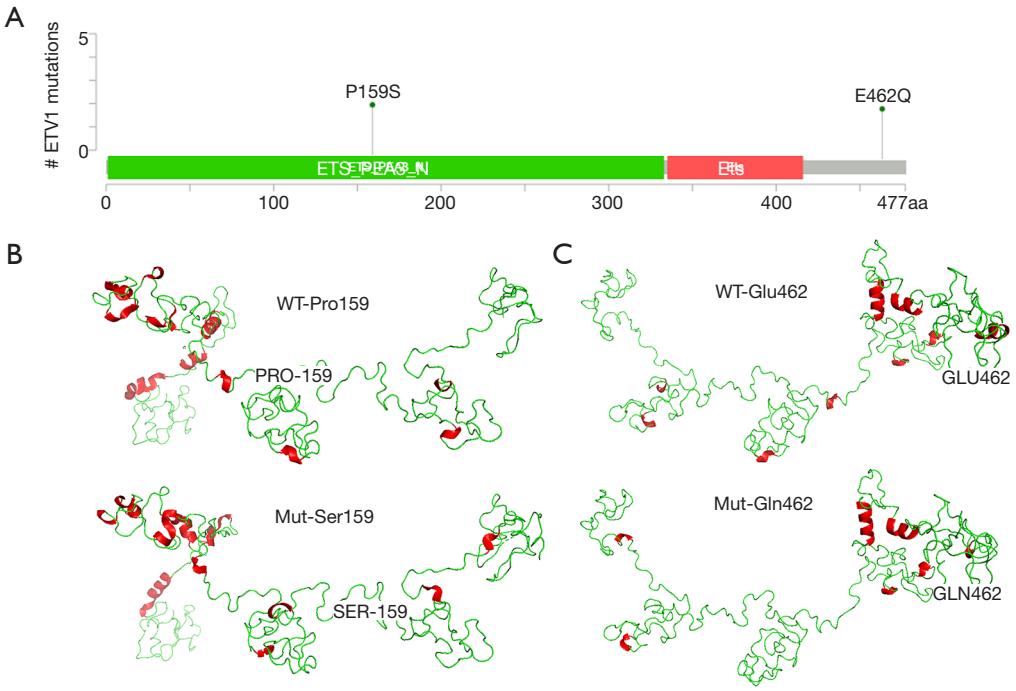

Figure 3 Structure domain and 3D protein structure diagrams of ETV1. (A) Two mutant sites were indicated in the structure of *ETV1*. (B,C) 3D protein structures of normal and mutant proteins of *ETV1*. Red means helix, green means sheet. ETV1, ETS variant transcription factor 1.

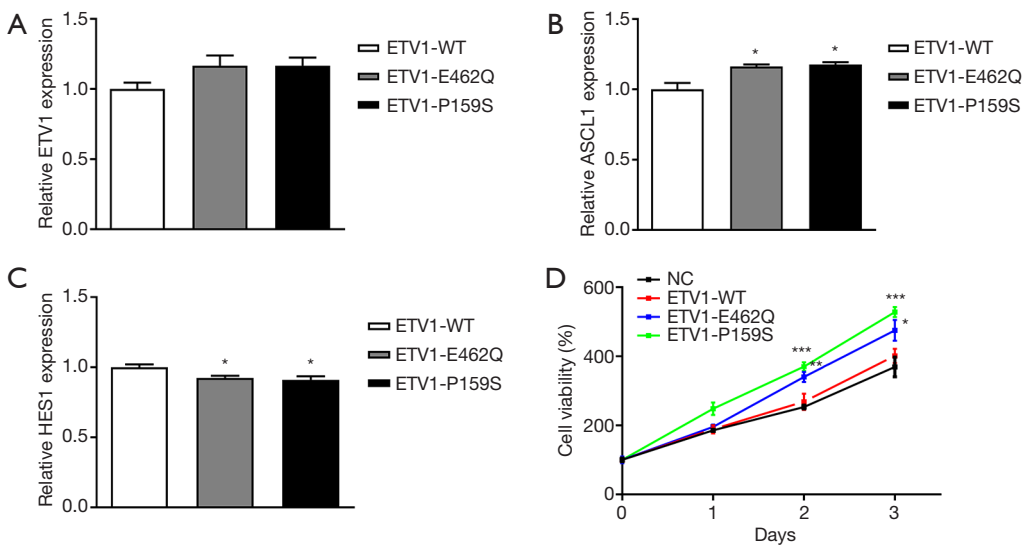

Figure 4 *ETV1* p.E462Q and p.P159S mutations promoted ASCL1 expression in SCLC. (A) Real time-PCR was used for the mRNA expression of *ETV1* after transfection of the *ETV1* WT and mutant plasmids. (B,C) ASCL1 and HES1 mRNA levels in cells transfected with *ETV1* mutant plasmids compared with those in cells transfected with the *ETV1* WT plasmid. (D) Cell proliferation of H69 cells after transfection of the *ETV1* WT and mutant plasmids. *, P<0.05; **, P<0.01; ***, P<0.001. ASCL1, achaete-scute homolog 1; SCLC, small cell lung cancer; ETV1, ETS variant transcription factor 1; WT, wild-type.

© Annals of Translational Medicine. All rights reserved.

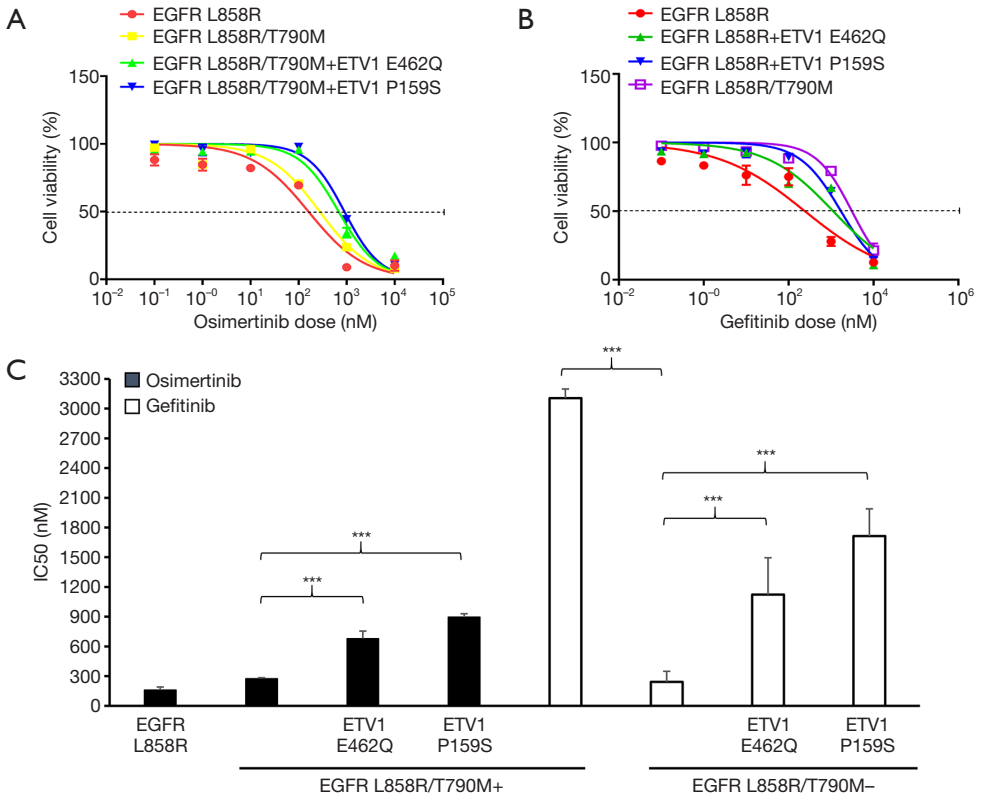

Figure 5 *ETV1* p.E462Q and p.P159S mutations induced gefitinib and osimertinib resistance *in vitro*. H358 cells harboring *EGFR* L858R and T790M plus indicated mutations were treated with osimertinib (A) or gefitinib (B) at the indicated concentrations. Cell viability was detected after 24 hours of treatment and plotted for comparison with untreated control cells. (C) IC50 values of different *EGFR* mutant cell lines to osimertinib and gefitinib treatment were plotted in bar graphs for comparison. Experiments were repeated twice in triplicate each time and the mean ± standard deviation value was plotted at each concentration. ***, P<0.001. EGFR, epidermal growth factor receptor; ETV1, ETS variant transcription factor 1.

is poor (18,19). The median survival time after confirmed transformation is 6–7 months (18). From a historical point of view, it is surprising that tumors could differentiate into NSCLC or SCLC at an early stage of tumorigenesis. *EGFR* mutant adenocarcinoma mainly occurs in people who never smoke, accompanied by a more sluggish natural process. Compared with NSCLC, SCLC almost always occurs in heavy smokers, and is prone to early metastasis and rapid growth (13,20).

In this study, repeated biopsies reminded us that SCLC transformed tumors might evolve from the initial adenocarcinoma rather than a concurrent cancer in the initial cases, because *EGFR* mutations in all cases were the same as those in the original LUAD. However, we could not rule out the possibility that SCLC with *EGFR* mutation existed before *EGFR*-TKI treatment, although we did not observe a mixed histology of NSCLC and SCLC in the tumor before treatment after carefully reviewing the histology of these two samples. However, from a clinical point of view, we suggested that these SCLCs were unlikely to exist in the early stage of tumorigenesis because classical SCLC develops very rapidly (13). *RB* expression loss and *TP53* mutation were deemed as the main molecular mechanisms involved in predicting SCLC transformation (21). After TKIs treatment, gene alterations accumulated, and EGFR signal that stimulated NSCLC differentiation was no longer necessary for proliferation, so cells differentiated into other lineages, including *EGFR* mutant SCLC. In addition, alveolar type II cells can produce *EGFR* mutant adenocarcinoma, but after *TP53* and *RB1* interfere with alveolar type II cells, SCLC appears. Other alterations such as *PTEN*, *CREBBP*, *SLIT2*, *EP300*,

© Annals of Translational Medicine. All rights reserved.

and *MLL* mutations, as well as *FGFR1* amplification have also been found in SCLC transformation cases (22,23). In view of these changes after *EGFR*-TKI exposure, resistant pluripotent stem cells subsequently differentiate into SCLC cells. Since these cells do not need EGFR signaling, they escape the influence of *EGFR*-TKI, so they will proliferate despite the presence of *EGFR*-TKI. Although there may be some EGFR mutations in transformed SCLC, the decrease or absent expression of EGFR may also lead to poor response to *EGFR*-TKI. The analysis of *EGFR* mutant tumor from adenocarcinoma to SCLC as acquired resistance mechanism showed that the lose protein expression of EGFR and the amplification level of EGFR was low. So, the response of *EGFR* mutant SCLC to *EGFR*-TKI does not seem to match those of *EGFR*-mutant adenocarcinoma. Thus, it is generally not recommended to detect *EGFR* mutations in SCLC. TKIs may not be effective in patients with SCLC due to the loss of EGFR expression at the protein level unless rare case had a positive EGFR mutation status, and they may respond to EGFR TKIs. In these two cases, *ETV1* alterations were particularly related to the transformation to SCLC, which provides new insight into the function of the *ETV1* gene and identifies a potential target that can be included in future treatment strategies for this type of cancer.

ETV1 is known as an oncogenic driver, and manifests as genomic translocation or amplification that causes aberrant E-twenty-six or E26 transformation-specific (ETS) expression in Ewing sarcoma, prostate cancer, and gastrointestinal stromal tumors, but not in lung cancer. In addition, *ETV1* fusion has been previously described in prostate cancer, melanoma, and Ewing sarcoma (24). Recently, *PTPRZ1-ETV1* and *DGKB-ETV1* fusion have also been detected in glioma (24,25). Herein, we first presented two cases in which *ETV1* mutations and neuroendocrine transformation exist together in the same lesion. Thus, to our knowledge, *ETV1* p.E462Q and p.P159S mutations detected in these two cases have not previously been reported in lung or other tumors. The prediction of the PROVEAN software (http://provean.jcvi.org) indicated that the mutant protein had a high score of pathogenicity and was a "deleterious" mutation, so these attracted our attention.

According to the LUAD data, there was no significant difference in the mutation frequency of *ETV1* between LUAD and SCLC, but there were fewer *ETV1* mutant cases reported in SCLC and the mutation was single. The mutation frequency of *ETV1* reported in the Asian population with LUAD was 1.37%, while that of European and Latin American populations was 2.73% and 1.71%, respectively. Only three SCLC patients with LUAD had the same *ETV1* mutation. However, there was no case report of *ETV1* mutations associated with SCLC type transition. All of these indicate that *ETV1* mutations are rare in lung cancer, however the role of *ETV1* gene in the occurrence and development of lung cancer is worth studying. In particular, computer simulation suggested that these two *ETV1* mutations might cause structural changes to the ETV1 protein, which may affect the normal function of enzyme activation and DNA binding.

The maintenance of the neuroendocrine phenotype of SCLC could be detected by the presence of neuroendocrine markers, such as ASCL1. The expression of ASCL1, which was obviously present in the SCLC components while being absent or rarely present in the LUAD, highlighted the vital role of ASCL1 in small cell transformation (26). In this study, *in vitro* experimentation showed that *ETV1* mutations increased the mRNA expression of ASCL1 in SCLC and promoted SCLC proliferation.

We also found that *ETV1* mutations could confer remarkable resistance to gefitinib and osimertinib. The *ETV1* p.E462Q variant exhibited mild resistance to osimertinib, while the *ETV1* p.E462Q and p.P159S variants showed strong resistance to gefitinib. Previous research has demonstrated that oncogenic ETV1/4/5 are targets of Capicua (CIC), a transcription factor downstream of the receptor tyrosine kinase and mitogen-activated protein kinase pathways, which have been found to play an important role in CIC loss mediating resistance to *EGFR* inhibition (27). *ETV1* expression is known to regulate ASCL1 expression via Notch signaling (28,29). We detected the expression levels of *HES1*, and suggested that *ETV1* mutations regulated the expression of ASCL1 through Notch, which may be proven in further study. Ultimately, there was no significant change in the ETV1 mRNA levels after transfection of the *ETV1* mutant plasmids. Collectively, these observations suggest the possibility that *ETV1* mutations may represent a mechanism of intrinsic resistance to *EGFR*-TKIs (*Figure 6*). Due to the heterogeneity of tumors, it is conceivable that multiple drug resistance mechanisms may exist simultaneously in a single patient, except for SCLC transformation.

The first-line standard chemotherapy is etoposide or irinotecan combined with platinum. Concurrent or sequential radiotherapy of the thorax and mediastinum is also necessary at a limited stage. If complete remission,

© Annals of Translational Medicine. All rights reserved.

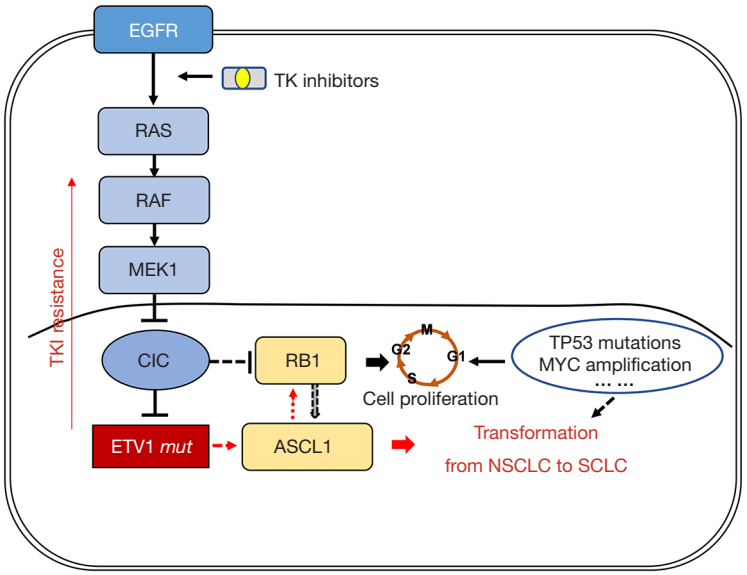

Figure 6 Molecular mechanisms of *ETV1* resistance to EGFR tyrosine kinase inhibitors in SCLC transformation. *ETV1* mutations stimulated EGFR signaling during gefitinib and osimertinib treatment and indirectly promoted ASCL1 overexpression, which contributed to neuroendocrine differentiation. EGFR, epidermal growth factor receptor; SCLC, small cell lung cancer; NSCLC, non-small cell lung cancer; *ETV1*, ETS variant transcription factor 1; ASCL1, achaete-scute homolog 1.

prophylactic cerebral irradiation (PCI) can prevent subsequent brain metastasis. In the extensive stage, chemotherapy is the main means of first-line treatment. SCLC is usually sensitive to initial treatment while most patients have recurrent disease and usually have additional metastases after initial treatment. Unfortunately, few drugs have been approved as effective second-line treatment for SCLC and the effects of them are not so good. In recent years, targeted therapy and immunotherapy have been actively tried. Nivolumab, the first FDA approved third-line treatment for SCLC, pembrolizumab, atezolizumab and durvalumab have achieved encouraging results. For other treatment options, the cytotoxic drug lurbinectedin was granted orphan drug. In addition, epigenetic inhibitors such as EZH1/2 inhibitors bring hope for the treatment of SCLC. The prospect of better treatment of SCLC lies in the combination of immunotherapy and small molecule TKI drugs. However, the success of this strategy will require the use of validated biomarkers to select the patients most likely to benefit from this strategy, including NGS for molecular alterations and a second biopsy to guide the next step of treatment and predict the prognosis.

This study highlights the importance of re-biopsy of progressive tumors in identifying a heterogeneous histopathological and genetic mechanism of resistance that might occur in *EGFR*-mutated NSCLCs when a rapid progression exists after an initial response. This will help clinicians to formulate the next stage of therapy, as the treatment of advanced LUAD and SCLC is completely different. In this study, the transformed SCLCs exhibited a good response to initial etoposide and cisplatin (EP) chemotherapy. Other drugs for transformed SCLC or other transformed subtypes need to be comprehensively explored in the future.

Conclusions

In this study, novel *ETV1* mutations were identified in two cases of *EGFR*-mutant LUAD that transformed to SCLC during treatment with first- and third-generation *EGFR*-TKIs. *ETV1* contributed to the promotion of neuroendocrine differentiation by stimulating ASCL1 expression and cell proliferation in SCLC. Moreover, *ETV1* could confer resistance to gefitinib and osimertinib *in vitro*. In future studies, the biological function of *ETV1* in lung cancer requires further exploration.

© Annals of Translational Medicine. All rights reserved.

Acknowledgments

We are particularly grateful to the participants in this research.

Funding: This work was supported by the Scientific Research Project of Shanghai Municipal Health Commission (201940084), the Beijing Medical and Health Foundation (YWJKJJHKYJJ-F2213E), and the Shanghai Sailing Program (20YF1444600).

Footnote

Reporting Checklist: The authors have completed the MDAR reporting checklist. Available at https://dx.doi.org/10.21037/atm-21-2625

Data Sharing Statement: Available at https://dx.doi.org/10.21037/atm-21-2625

Conflicts of Interest: All authors have completed the ICMJE uniform disclosure form (available at https://dx.doi.org/10.21037/atm-21-2625). WYX reports that she was employed by company Singlera Genomics (Shanghai) Ltd. The other authors have no conflicts of interest to declare.

Ethical Statement: The authors are accountable for all aspects of the work in ensuring that questions related to the accuracy or integrity of any part of the work are appropriately investigated and resolved. All procedures performed in this study involving human participants were in accordance with the Declaration of Helsinki (as revised in 2013). The study was approved by Research Ethics Committee of Shanghai Chest Hospital (IS2118) and informed consent was taken from all the patients.

Open Access Statement: This is an Open Access article distributed in accordance with the Creative Commons Attribution-NonCommercial-NoDerivs 4.0 International License (CC BY-NC-ND 4.0), which permits the non-commercial replication and distribution of the article with the strict proviso that no changes or edits are made and the original work is properly cited (including links to both the formal publication through the relevant DOI and the license). See: https://creativecommons.org/licenses/by-nc-nd/4.0/.

References

1. Jemal A, Bray F, Center MM, et al. Global cancer statistics. CA Cancer J Clin 2011;61:69-90.
2. Bade BC, Dela Cruz CS. Lung Cancer 2020: Epidemiology, Etiology, and Prevention. Clin Chest Med 2020;41:1-24.
3. Chen HF, Lei L, Wu LX, et al. Effect of icotinib on advanced lung adenocarcinoma patients with sensitive EGFR mutation detected in ctDNA by ddPCR. Transl Cancer Res 2019;8:2858-63.
4. Novello S, Barlesi F, Califano R, et al. Metastatic non-small-cell lung cancer: ESMO Clinical Practice Guidelines for diagnosis, treatment and follow-up. Ann Oncol 2016;27:v1-v27.
5. Jackman D, Pao W, Riely GJ, et al. Clinical definition of acquired resistance to epidermal growth factor receptor tyrosine kinase inhibitors in non-small-cell lung cancer. J Clin Oncol 2010;28:357-60.
6. Facchinetti F, Proto C, Minari R, et al. Mechanisms of Resistance to Target Therapies in Non-small Cell Lung Cancer. Handb Exp Pharmacol 2018;249:63-89.
7. Buder A, Hochmair MJ, Setinek U, et al. EGFR mutation tracking predicts survival in advanced EGFR-mutated non-small cell lung cancer patients treated with osimertinib. Transl Lung Cancer Res 2020;9:239-45.
8. Mok TS, Wu YL, Ahn MJ, et al. Osimertinib or Platinum-Pemetrexed in EGFR T790M-Positive Lung Cancer. N Engl J Med 2017;376:629-40.
9. Bordi P, Del Re M, Minari R, et al. From the beginning to resistance: Study of plasma monitoring and resistance mechanisms in a cohort of patients treated with osimertinib for advanced T790M-positive NSCLC. Lung Cancer 2019;131:78-85.
10. Mu Y, Hao X, Xing P, et al. Acquired resistance to osimertinib in patients with non-small-cell lung cancer: mechanisms and clinical outcomes. J Cancer Res Clin Oncol 2020;146:2427-33.
11. Ren X, Cai X, Li J, et al. Histological transformation of lung adenocarcinoma to small cell lung cancer with mutant C797S conferring acquired resistance to osimertinib. J Int Med Res 2020;48:300060520927918.
12. Oser MG, Niederst MJ, Sequist LV, et al. Transformation from non-small-cell lung cancer to small-cell lung cancer: molecular drivers and cells of origin. Lancet Oncol 2015;16:e165-72.
13. Sequist LV, Waltman BA, Dias-Santagata D, et al. Genotypic and histological evolution of lung cancers acquiring resistance to EGFR inhibitors. Sci Transl Med 2011;3:75ra26.
14. Watanabe S, Sone T, Matsui T, et al. Transformation

© Annals of Translational Medicine. All rights reserved.

to small-cell lung cancer following treatment with EGFR tyrosine kinase inhibitors in a patient with lung adenocarcinoma. Lung Cancer 2013;82:370-2.
15. Offin M, Chan JM, Tenet M, et al. Concurrent RB1 and TP53 Alterations Define a Subset of EGFR-Mutant Lung Cancers at risk for Histologic Transformation and Inferior Clinical Outcomes. J Thorac Oncol 2019;14:1784-93.
16. Sementchenko VI, Watson DK. Ets target genes: past, present and future. Oncogene 2000;19:6533-48.
17. Yu HA, Arcila ME, Rekhtman N, et al. Analysis of tumor specimens at the time of acquired resistance to EGFR-TKI therapy in 155 patients with EGFR-mutant lung cancers. Clin Cancer Res 2013;19:2240-7.
18. Roca E, Gurizzan C, Amoroso V, et al. Outcome of patients with lung adenocarcinoma with transformation to small-cell lung cancer following tyrosine kinase inhibitors treatment: A systematic review and pooled analysis. Cancer Treat Rev 2017;59:117-22.
19. Ma S, He Z, Fu H, et al. Dynamic changes of acquired T790M mutation and small cell lung cancer transformation in a patient with EGFR-mutant adenocarcinoma after first- and third-generation EGFR-TKIs: a case report. Transl Lung Cancer Res 2020;9:139-43.
20. Basumallik N, Agarwal M. Small Cell Lung Cancer. StatPearls. Treasure Island, FL; 2020.
21. Lee JK, Lee J, Kim S, et al. Clonal History and Genetic Predictors of Transformation Into Small-Cell Carcinomas From Lung Adenocarcinomas. J Clin Oncol 2017;35:3065-74.
22. Forgacs E, Biesterveld EJ, Sekido Y, et al. Mutation analysis of the PTEN/MMAC1 gene in lung cancer. Oncogene 1998;17:1557-65.
23. Peifer M, Fernández-Cuesta L, Sos ML, et al. Integrative genome analyses identify key somatic driver mutations of small-cell lung cancer. Nat Genet 2012;44:1104-10.
24. Johnson A, Severson E, Gay L, et al. Comprehensive Genomic Profiling of 282 Pediatric Low- and High-Grade Gliomas Reveals Genomic Drivers, Tumor Mutational Burden, and Hypermutation Signatures. Oncologist 2017;22:1478-90.
25. Matjasic A, Zupan A, Bostjancic E, et al. A novel PTPRZ1-ETV1 fusion in gliomas. Brain Pathol 2020;30:226-34.
26. Lin MW, Su KY, Su TJ, et al. Clinicopathological and genomic comparisons between different histologic components in combined small cell lung cancer and non-small cell lung cancer. Lung Cancer 2018;125:282-90.
27. Liao S, Davoli T, Leng Y, et al. A genetic interaction analysis identifies cancer drivers that modify EGFR dependency. Genes Dev 2017;31:184-96.
28. Akazawa C, Sasai Y, Nakanishi S, et al. Molecular characterization of a rat negative regulator with a basic helix-loop-helix structure predominantly expressed in the developing nervous system. J Biol Chem 1992;267:21879-85.
29. Kovach C, Dixit R, Li S, et al. Neurog2 simultaneously activates and represses alternative gene expression programs in the developing neocortex. Cereb Cortex 2013;23:1884-900.

(English Language Editor: A. Kassem)

Cite this article as: Zhou Y, Bai H, Xia J, Xu WY, Cheng L, Xiong L. Novel ETV1 mutation in small cell lung cancer transformation resistant to EGFR tyrosine kinase inhibitors. Ann Transl Med 2021;9(14):1150. doi: 10.21037/atm-21-2625

© Annals of Translational Medicine. All rights reserved.

Table S1 Genes list of the 639 DNA panel

ABCB1	BRD4	COL5A1	EPCAM	FGFR3	HIST3H3	KMT2B	MSI2	PCNA	PTPRT	SETD8	TEK	ZFHX3
ABCB9	BRIP1	CREBBP	EPHA3	FGFR4	HLA-A	KMT2C	MST1	PDCD1	QKI	SF3B1	TERT	ZNF217
ABL1	BTG1	CRKL	EPHA5	FH	HLA-B	KMT2D	MST1R	PDCD1LG2	RAB35	SGK1	TET1	ZNF703
ABL2	BTG2	CRLF2	EPHA7	FLCN	HLA-C	KNSTRN	MTAP	PDGFRA	RAC1	SH2B3	TET2	
ACE2	BTK	CSDE1	EPHB1	FLT1	HLA-DRB1	KRAS	MTHFR	PDGFRB	RAC2	SH2D1A	TGFBR1	
ACVR1	C10orf54	CSF1R	EPHB4	FLT3	HMGB1	LATS1	MTOR	PDIA3	RAD21	SHOC2	TGFBR2	
ACVR1B	C11orf30	CSF3R	EPHX1	FLT4	HMGN1	LATS2	MTRR	PDK1	RAD50	SHQ1	TIPARP	
AGO2	C8orf34	CTCF	ERAP1	FOXA1	HNF1A	LGALS9	MUTYH	PDPK1	RAD51	SLC34A2	TMEM127	
AKT1	CALR	CTLA4	ERAP2	FOXL2	HOXB13	LGMN	MYB	PGR	RAD51B	SLCO1B1	TMPRSS2	
AKT2	CANX	CTNNA1	ERBB2	FOXO1	HRAS	LIG1	MYC	PHF6	RAD51C	SLIT2	TNF	
AKT3	CARD11	CTNNB1	ERBB3	FOXP1	HSD3B1	LIG3	MYCL	PHOX2B	RAD51D	SLX4	TNFAIP3	
ALK	CARM1	CTSB	ERBB4	FRS2	HSP90AA1	LMO1	MYCN	PIK3C2B	RAD52	SMAD2	TNFRSF14	
ALOX12B	CASP8	CTSL	ERCC1	FUBP1	ICOSLG	LNPEP	MYD88	PIK3C2G	RAD54L	SMAD3	TNFRSF9	
AMER1	CBFB	CTSS	ERCC2	FYN	ID3	LRP1B	MYOD1	PIK3C3	RAF1	SMAD4	TNFSF14	
ANKRD11	CBL	CUL3	ERCC3	GABRA6	IDE	LTK	NBN	PIK3CA	RANBP2	SMARCA4	TNFSF18	
APC	CBR3	CUL4A	ERCC4	GATA1	IDH1	LYN	NCOA3	PIK3CB	RARA	SMARCB1	TNFSF4	
AR	CCND1	CXCR4	ERCC5	GATA2	IDH2	LZTR1	NCOR1	PIK3CD	RASA1	SMARCD1	TNFSF9	
ARAF	CCND2	CYLD	ERF	GATA3	IFI30	MAF	NEGR1	PIK3CG	RB1	SMO	TOP1	
ARFRP1	CCND3	CYP17A1	ERG	GATA4	IFNGR1	MAGI2	NF1	PIK3R1	RBM10	SMYD3	TOP2A	
ARID1A	CCNE1	CYP19A1	ERRFI1	GATA6	IGF1	MALT1	NF2	PIK3R2	RECQL	SNCAIP	TP53	
ARID1B	CD200	CYP2C19	ESR1	GID4	IGF1R	MAP2K1	NFE2L2	PIK3R3	RECQL4	SOCS1	TP53BP1	
ARID2	CD22	CYP2C8	ETV1	GLI1	IGF2	MAP2K2	NFKBIA	PIM1	REL	SOD2	TP63	
ARID5B	CD274	CYP2C9	ETV4	GNA11	IKBKE	MAP2K4	NKX2-1	PLCG2	RET	SOS1	TP73	
ASXL1	CD276	CYP2D6	ETV5	GNA13	IKZF1	MAP3K1	NKX3-1	PLK2	RFWD2	SOX10	TPMT	
ASXL2	CD40	CYP3A4	ETV6	GNAQ	IL10	MAP3K13	NOTCH1	PMAIP1	RHEB	SOX17	TPP2	
ATM	CD40LG	CYSLTR2	EWSR1	GNAS	IL7R	MAP3K14	NOTCH2	PMS1	RHOA	SOX2	TRAF2	
ATR	CD48	DAXX	EXO1	GPR124	INHA	MAPK1	NOTCH3	PMS2	RICTOR	SOX9	TRAF7	
ATRX	CD70	DCUN1D1	EZH1	GPS2	INHBA	MAPK3	NOTCH4	PNRC1	RIT1	SPEN	TSC1	
AURKA	CD74	DDR1	EZH2	GREM1	INPP4A	MAPKAP1	NPEPPS	POLB	RNF43	SPOP	TSC2	
AURKB	CD79A	DDR2	EZR	GRIN2A	INPP4B	MAX	NPM1	POLD1	ROS1	SPRED1	TSHR	
AXIN1	CD79B	DHFR	FAM175A	GRM3	INPPL1	MCL1	NQO1	POLE	RPS6KA4	SPTA1	TYMS	
AXIN2	CD80	DICER1	FAM46C	GSK3B	INSR	MDC1	NRAS	PPARG	RPS6KB2	SRC	TYRO3	
AXL	CD86	DIS3	FAM58A	GSTP1	IRF2	MDM2	NRD1	PPM1D	RPTOR	SRSF2	U2AF1	
B2M	CDA	DMD	FANCA	H3F3A	IRF4	MDM4	NSD1	PPP2R1A	RRAGC	STAG2	UGT1A1	
BABAM1	CDC42	DNAJB1	FANCC	H3F3B	IRS1	MED12	NT5C2	PPP2R2A	RRAS	STAT3	UGT1A9	
BAP1	CDC73	DNMT1	FANCD2	H3F3C	IRS2	MEF2B	NTHL1	PPP4R2	RRAS2	STAT4	UPF1	
BARD1	CDH1	DNMT3A	FANCE	HDAC1	ITGAV	MEN1	NTRK1	PPP6C	RRM1	STAT5A	VEGFA	
BBC3	CDK12	DNMT3B	FANCF	HERC1	ITGB3	MERTK	NTRK2	PRDM1	RSPO2	STAT5B	VHL	
BCL10	CDK4	DOT1L	FANCG	HGF	JAK1	MET	NTRK3	PRDM14	RTEL1	STK11	VTCN1	
BCL2	CDK6	DPYD	FANCL	HIST1H1C	JAK2	MGA	NUF2	PREX2	RUNX1	STK19	WHSC1	
BCL2L1	CDK8	DROSHA	FAS	HIST1H2BD	JAK3	MICA	NUP93	PRKAR1A	RUNX1T1	STK40	WHSC1L1	
BCL2L11	CDKN1A	DUSP4	FAT1	HIST1H3A	JUN	MICB	NUTM1	PRKCI	RXRA	SUFU	WISP3	
BCL2L2	CDKN1B	DYNC2H1	FBXW7	HIST1H3B	KAT6A	MITF	P2RY8	PRKD1	RYBP	SUZ12	WT1	
BCL6	CDKN2A	E2F3	FGF10	HIST1H3C	KDM5A	MKNK1	PAK1	PRKDC	SDC4	SYK	WWTR1	
BCOR	CDKN2B	EED	FGF12	HIST1H3D	KDM5C	MLH1	PAK3	PRSS8	SDHA	TAF1	XIAP	
BCORL1	CDKN2C	EGFL7	FGF14	HIST1H3E	KDM6A	MLH3	PAK7	PTCH1	SDHAF2	TAP1	XPC	
BCR	CEBPA	EGFR	FGF19	HIST1H3F	KDR	MPL	PALB2	PTEN	SDHB	TAP2	XPO1	
BIRC3	CENPA	EIF1AX	FGF23	HIST1H3G	KEAP1	MRE11	PARK2	PTGS2	SDHC	TAPBP	XRCC1	
BLM	CHD2	EIF4A2	FGF3	HIST1H3H	KEL	MRE11A	PARP1	PTP4A1	SDHD	TAPBPL	XRCC2	
BMPR1A	CHD4	EIF4E	FGF4	HIST1H3I	KIT	MSH2	PARP2	PTPN11	SESN1	TBX3	XRCC5	
BRAF	CHEK1	ELF3	FGF6	HIST1H3J	KLF4	MSH3	PARP3	PTPRD	SESN2	TCEB1	YAP1	
BRCA1	CHEK2	EP300	FGFR1	HIST2H3C	KLHL6	MSH6	PAX5	PTPRO	SESN3	TCF3	YES1	
BRCA2	CIC	EPAS1	FGFR2	HIST2H3D	KMT2A	MSI1	PBRM1	PTPRS	SETD2	TCF7L2	ZBTB2	

The DNA panel is a hybridization capture-based NGS panel to detect single nucleotide variants (SNVs), insertion and deletion alterations (InDels), and copy number alterations (CNAs) involved in 639 cancer-associated genes in tumors. This panel is designed to provide mutation profiling of patients with solid tumors.

© Annals of Translational Medicine. All rights reserved.
https://dx.doi.org/10.21037/atm-21-2625

Table S2 Primer sequences list

Primer	Sequences (5'→3')
H-GAPDH-F	GGAGCGAGATCCCTCCAAAAT
H-GAPDH-R	GGCTGTTGTCATACTTCTCATGG
H-ETV1-F	TGGCAGTTTTTGGTAGCTCTTC
H-ETV1-R	CGGAGTGAACGGCTAAGTTTATC
H-NOTCH1-F	TGGACCAGATTGGGGAGTTC
H-NOTCH1-R	GCACACTCGTCTGTGTTGAC
H-NOTCH2-F	CCTTCCACTGTGAGTGTCTGA
H-NOTCH2-R	AGGTAGCATCATTCTGGCAGG
H-ASCL1-F	CGCGGCCAACAAGAAGATG
H-ASCL1-R	CGACGAGTAGGATGAGACCG
H-HES1-F	CCTGTCATCCCCGTCTACAC
H-HES1-R	CACATGGAGTCCGCCGTAA
EGFR-WT-F	CTCGGATCCGCCACCATGCGACCCTCCGGGACGGC
EGFR-WT-R	CCCTCTAGACTCGAGTGCTCCAATAAATTCACTGCTT
EGFR-L858R -F	CTCGGATCCGCCACCATGCGACCCTCCGGGACGGC
EGFR-L858R -R	CCCTCTAGACTCGAGTGCTCCAATAAATTCACTGCTT
EGFR-T790M -F	CTCGGATCCGCCACCATGCGACCCTCCGGGACGGC
EGFR-T790M -R	CCCTCTAGACTCGAGTGCTCCAATAAATTCACTGCTT
ETV1-WT-F	CTCGGATCCGCCACCATGGATGGATTTTATGACCAG
ETV1-WT-R	CCCTCTAGACTCGAGATACACGTAGCCTTCGTTGTA
ETV1-E462Q-F	CTCGGATCCGCCACCATGGATGGATTTTATGACCAG
ETV1-E462Q-R	CCCTCTAGACTCGAGATACACGTAGCCTTCGTTGT
ETV1-P159S-F	CTCGGATCCGCCACCATGGATGGATTTTATGACCAG
ETV1-P159S-R	CCCTCTAGACTCGAGATACACGTAGCCTTCGTTGT

© Annals of Translational Medicine. All rights reserved.
https://dx.doi.org/10.21037/atm-21-2625

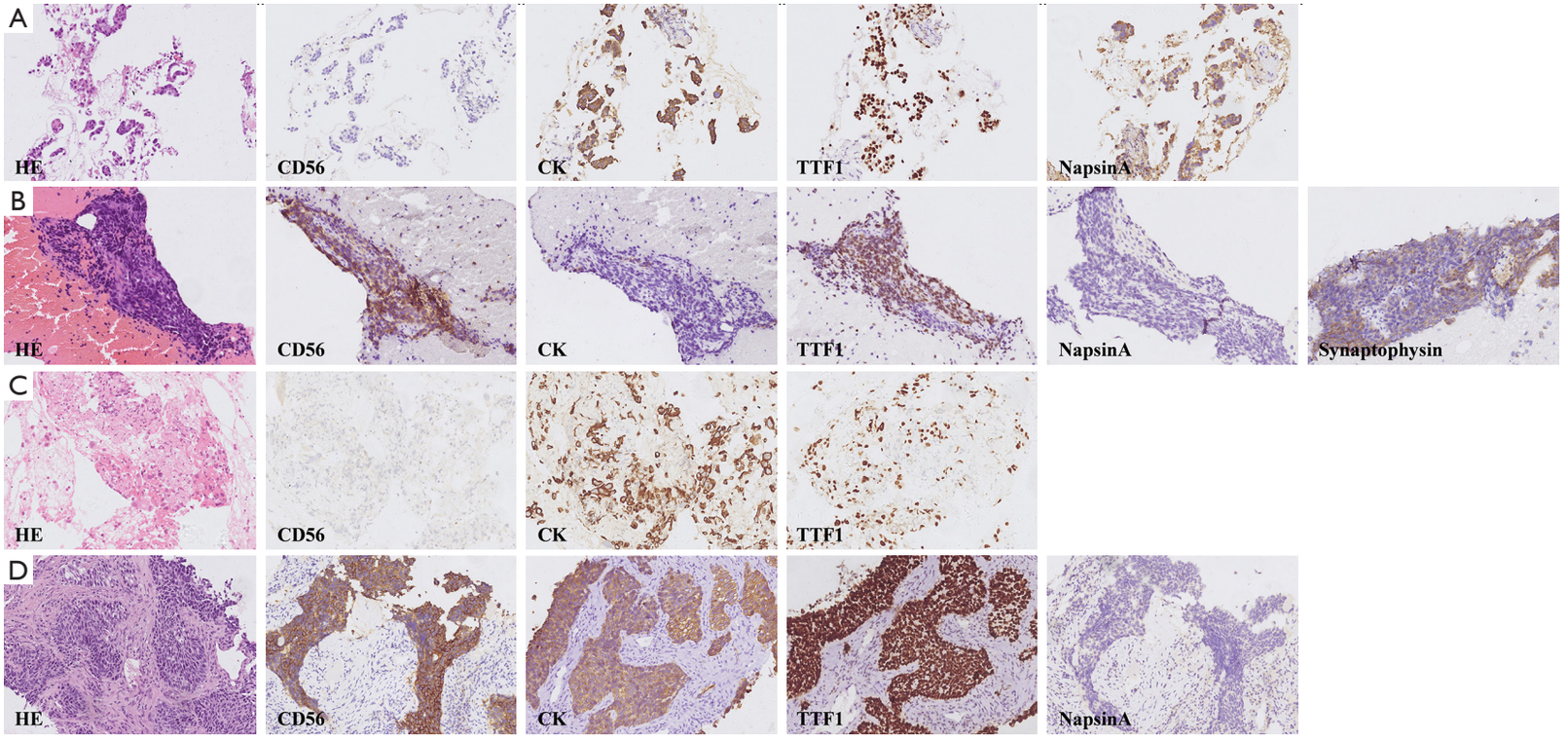

Figure S1 Pathological findings of the patients. (A) LUAD histology of case 1 before osimertinib treatment. IHC was strongly positive for CK, TTF1, and NapsinA, and negative for CD56 (200×). (B) Hematoxylin & eosin staining showed that the cells were SCLC phenotype. IHC was positive for CD56 and synaptophysin, +/– for CK, partially positive for TTF1, and negative for NapsinA (200×). (C) LUAD histology of case 2 before *EGFR*-TKI treatment. IHC was strongly positive for CK and TTF1, and negative for CD56 (200×). (D) Re-biopsy after TKI resistance showed SCLC transformation. IHC was positive for CD56, CK, TTF1, and NapsinA (200×).

© Annals of Translational Medicine. All rights reserved.
https://dx.doi.org/10.21037/atm-21-2625

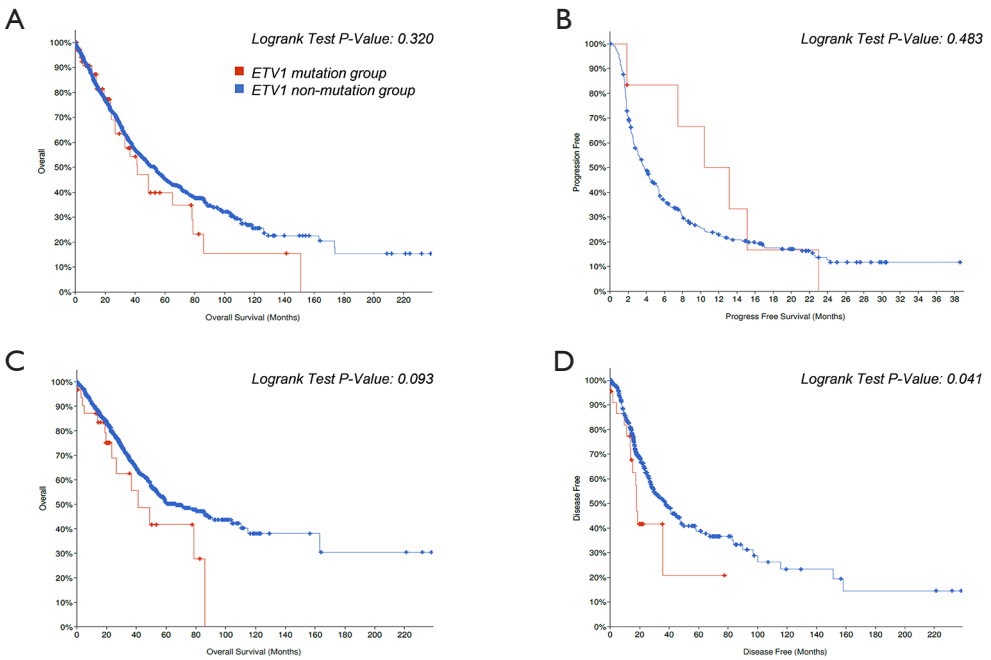

Figure S2 Survival association analysis of *ETV1* mutations. (A) Kaplan-Meier OS analysis for tumor patients with and without *ETV1* mutations in the TCGA cohorts. (B) PFS for tumor patients with and without *ETV1* mutations. (C,D) OS and DFS analysis for LUAD patients with and without *ETV1* mutations.

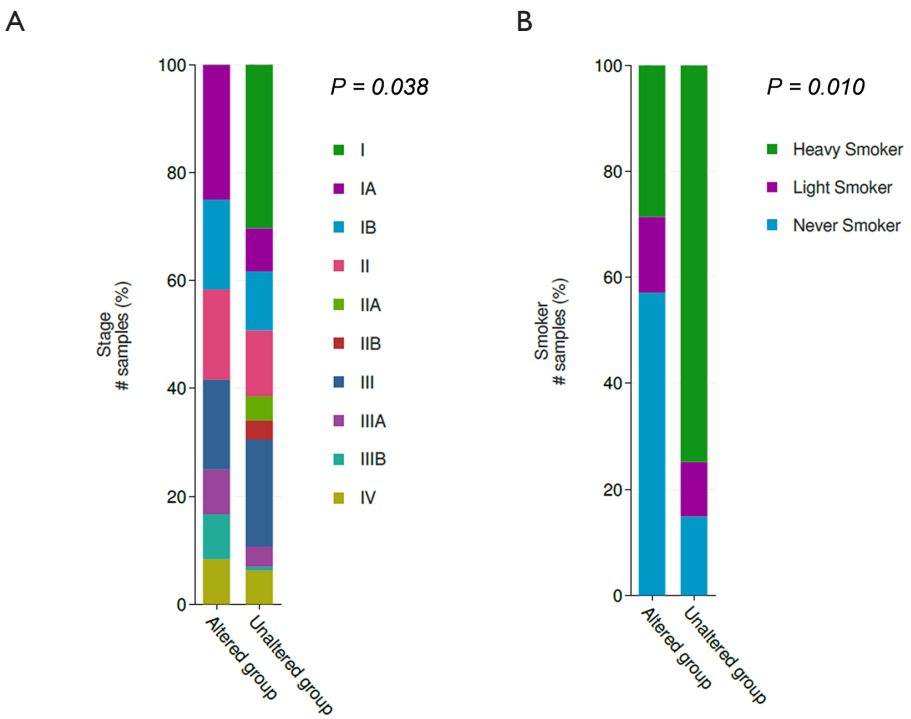

Figure S3 Clinical correlation analysis of *ETV1* mutations. (A) Comparison of tumor stage between *ETV1* mutated and non-mutated LUAD. (B) Smoking status and *ETV1* mutations.

© Annals of Translational Medicine. All rights reserved.
https://dx.doi.org/10.21037/atm-21-2625